Jakes, K. S., & Zinder, N. D. (1974) *Proc. Natl. Acad. Sci. U.S.A. 74*, 3380-3384.
Jeener, J., Meier, B. H., Bachmann, P., & Ernst, R. R. (1979) *J. Chem. Phys. 71*, 4546-4533.
Kay, L. E., & Bax, A. (1990) *J. Magn. Reson. 86*, 110-126.
MacIntosh, L. P., Wand, A. J., Lowry, D. F., Redfield, A. G., & Dahlquist, F. W. (1990) *Biochemistry 29*, 6341-6362.
Macura, S., Huang, Y., Suter, D., & Ernst, R. R. (1981) *J. Magn. Reson. 43*, 259-281.
Marion, D., & Wüthrich, K. (1983) *Biochem. Biophys. Res. Commun. 113*, 967-974.
Masaki, H., & Ohta, T. (1982) *FEBS Lett. 149*, 129-132.
Masaki, H., & Ohta, T. (1985) *J. Mol. Biol. 182*, 217-227.
Masaki, H., Akutsu, A., & Ohta, T. (1991) *Gene 107*, 133-138.
Messing, J., (1983) *Methods Enzymol. 101*, 20-78.
Mochitate, K., Suzuki, K., & Imahori, K. (1981) *J. Biochem. (Tokyo) 89*, 1609-1618.
Mueller, L. (1979) *J. Am. Chem. Soc. 101*, 4481-4484.
Ohno, S., & Imahori, K. (1978) *J. Biochem. (Tokyo) 84*, 1637-1640.
Ohno-Iwashita, Y., & Imahori, K. (1980) *Biochemistry 19*, 652-659.
Piatini, U., Sørenson, O. W., & Ernst, R. R. (1982) *J. Am. Chem. Soc. 104*, 7310-7311.
Plateau, P., & Gueron, M. (1982) *J. Am. Chem. Soc. 104*, 7310-7311.
Pugsley, A. P., & Oudega, B. (1987) *Plasmids: A Practical Approach*, IRL Press, Oxford.
Rance, M., Sørensen, O. W., Bodenhausen, G., Wagner, G., Ernst, R. R., & Wüthrich, K. (1983) *Biochem. Biophys. Res. Commun. 117*, 479-485.
Redfield, A. G. (1983) *Chem. Phys. Lett. 96*, 537-540.
Redfield, A. G., & Kuntz, S. D. (1975) *J. Magn. Reson. 19*, 250-254.
Skelnar, V., & Bax, A. (1987) *J. Magn. Reson. 71*, 379-383.
Suzuki, K., & Imahori, K. (1978) *J. Biochem. (Tokyo) 84*, 1031-1039.
Toba, M., Masaki, H., & Ohta, T. (1986) *J. Biochem. (Tokyo) 99*, 591-596.
Torchia, D. A., Sparks, S. W., & Bax, A. (1989) *Biochemistry 28*, 5509-5524.
Wang, J., Hinck, A. P., Loh, S. N., & Markley, J. L. (1990) *Biochemistry 29*, 102-113.
Wüthrich, K. (1986) *NMR of Proteins and Nucleic Acids*, Wiley, New York.
Yamasaki, K., Kawai, G., Ito, Y., Muto, Y., Fujita, J., Miyazawa, T., Nishimura, S., & Yokoyama, S. (1989) *Biochem. Biophys. Res. Commun. 162*, 1054.
Yamasaki, K., Muto, Y., Ito, Y., Wälchili, M., Miyazawa, T., Nishimura, S., & Yokoyama, S. (1992) *J. Biomol. NMR* (in press).
Yanisch-Perron, C., Vieira, J., & Messing, J. (1985) *Gene 33*, 103-119.

Fluorenyl Fatty Acids as Fluorescent Probes for Depth-Dependent Analysis of Artificial and Natural Membranes†

Anil K. Lala* and Vishwanath Koppaka
Biomembrane Lab, Department of Chemistry, Indian Institute of Technology Bombay, Powai, Bombay 400076, India
Received October 2, 1991; Revised Manuscript Received March 18, 1992

ABSTRACT: The main objective of depth-dependent fluorescent probes is to provide information at a distinct position in the membrane hydrophobic core. We report here a series of fluorenyl fatty acids which can probe both artificial and natural membranes at different depths. Long-chain acids (C4, C6, and C8) are attached to fluorene chromophore on one side, and a hydrophobic tail (C4) is attached on the other side, so that on incorporation in membranes the carboxyl end of the molecule is oriented toward the membrane–water interface and the hydrophobic tail points toward the membrane interior. These acids can be readily partitioned into membranes. The disposition of these fluorenyl fatty acids in membranes was studied by fluorescence quenching using iodide as a water-soluble and 9,10-dibromostearic acid as a lipid-soluble quencher. The results obtained indicate that attachment of a hydrophobic tail is essential for effective alignment of depth-dependent fluorescent probes. The length of the hydrophobic tail was varied and an *n*-butyl chain was found to be most effective. In all cases, the compounds with a hydrophobic tail were found to be probing the membrane deeper than their counterparts with no hydrophobic tail. Further, the compounds with hydrophobic tails were more strongly immobilized in the membrane as indicated by fluorescence polarization studies. However, the effect of such a tail varied with membrane type. Thus in artificial membranes an *n*-butyl chain was found to be extremely important for effective monitoring by shallow probes like 4-(2′-fluorenyl)butyric acid, whereas in erythrocyte ghost membranes the same *n*-butyl tail was found to be more desirable for deeper probes like 8-(2′-fluorenyl)octanoic acid. The general molecular design strategy reported here can be extended to other fluorescent probes and photoactivable reagents for depth-dependent analysis of membranes.

The main objective of depth-dependent analysis of membranes is to provide information at different depths. Fluorescent probes have been frequently used toward this end (Blatt & Sawyer, 1985). Both fluorescent fatty acids and phospholipids have been used in this context. The most notable in this class have been the *n*-anthroyloxy fatty acids (Thulborn & Sawyer, 1978), pyrenyl fatty acids (Waka et al., 1980; Jones & Lentz, 1986), and anthracene fatty acids (de Bony & To-

† This work was supported by a grant-in-aid from the Department of Science and Technology, Delhi, India.
* Author to whom correspondence should be addressed.

0006-2960/92/0431-5586$03.00/0

canne, 1983; Vincent et al., 1985; Molotkovsky, 1984). We have recently reported the use of fluorenyl fatty acids for depth-dependent analysis of membranes (Lala et al., 1988). A suitable molecular design criterion was developed to get over any problems associated with looping back of these fluorescent probes to the membrane–water interface. According to this design criterion, attachment of a hydrophobic tail to a substituted fatty acid like 4-(2′-fluorenyl)butyric acid (C4A-FL),[1] resulting in 4-(2′-fluoren-7′-butyl)butyric acid (C4A-FL-C4), assists in better alignment of the fluorescent probe (Lala et al., 1988). However, these studies were restricted to artificial membranes. In this paper we report several new fluorenyl fatty acids which confirm the validity of the molecular design criterion mentioned above and further show that these probes can be successfully used for depth-dependent fluorescence analysis in both artificial and natural membranes.

Materials and Methods

Chemical Synthesis. All chemicals and solvents were commercial grades of highest purity available and were further purified, if required, according to Perrin et al. (1980). UV–visible spectra were recorded on a Shimadzu UV-265 spectrophotometer. IR spectra were recorded on a Perkin-Elmer 691 spectrophotometer. NMR spectra were recorded either on a Varian 300-MHz spectrometer or a Bruker 500-MHz spectrometer. Mass spectra were recorded on a Shimadzu QP 1000 spectrometer. High-pressure liquid chromatography was carried out on a Shimadzu LC-6A liquid chromatograph using a Shimpak CLC-ODS column (6 × 150 mm) and a SPD-2AS UV monitor interfaced to CR-3A integrator. Methanol/water (95:5, v/v) was used as eluent with a flow rate of 1 mL/min. The eluant was monitored at 260 nm. Gas chromatography was carried out on a Shimadzu GC 9A instrument using a Shimadzu SE 30 (1.5%, glass spiral column, 3 × 1100 mm, support chromosorb W 60–80 mesh) column and a flame ionization detector. Helium was used as the carrier gas with a flow rate of 40 mL/min. The injection port was maintained at 190 °C. The column temperature was programmed as follows: It was initially maintained at 190 °C, and after 2 min the temperature was gradually raised at a rate of 2 °C/min up to 240 °C. Fluorescence spectra were recorded on a Shimadzu RF 540 fluorescence spectrometer. All the melting points reported are uncorrected.

4-(2′-Fluorenyl)butyric acid (I, C4A-FL), 6-(2′-fluorenyl)hexanoic acid (V, C6A-FL), 8-(2′-fluorenyl)octanoic acid (III, C8A-FL), and 4-(2′-fluoren-7′-butyl)butyric acid (II, C4A-FL-C4) were prepared as reported earlier (Lala et al., 1988). 6-(2′-Fluoren-7′-acetyl)hexanoic acid (VI, C6A-FL-C2) was also prepared as reported earlier (Anjaneyulu & Lala, 1988). We are thankful to Dr. Rajiv R. Dixit for providing 6-(2′-fluoren-7′-butyl)-hexanoic acid (VII, C6A-FL-C4).

8-(2′-Fluoren-7′-butyl)octanoic Acid (IV, C8A-FL-C4). 2-*n*-Butylfluorene was prepared as described earlier (Lala et al., 1988). Briefly, fluorene was acylated with butyric anhydride to get 2-*n*-butyroyl fluorene according to the procedure of Buu Hoi and Cagniant (1946) which was then converted to 2-*n*-butylfluorene by Wolff–Kishner reduction according to the procedure of Huang (1946). Dry 2-*n*-butylfluorene (1.3 g, 5.5 mmol) was dissolved in dry carbon disulfide (7 mL) and stirred. Anhydrous aluminum chloride (2.1 g, 0.16 mol) was then added in portions. Freshly prepared methyl suberoyl chloride (1.54 g, 6.5 mmol) in dry carbon disulfide (3 mL) was added dropwise over a period of 1 h and then refluxed for 6 h. The excess of carbon disulfide was distilled, and the complex was washed with more carbon disulfide and petroleum ether. The aluminum chloride complex was then hydrolyzed by adding the complex into ice-cold dilute hydrochloric acid. It was stirred at room temperature for 4 h to ensure complete hydrolysis and then extracted with chloroform. The chloroform layer was washed with 10% sodium bicarbonate solution, water, and saturated solution of sodium chloride and dried over anhydrous sodium sulfate and filtered. The chloroform was distilled off on a water bath and crude material so obtained was subjected to silica gel (60 g) column chromatography and eluted with 80% chloroform in petroleum ether to give the ester which was crystallized from benzene–petroleum ether to give pure 8-(2′-fluoren-7′-butyl)-7-oxooctanoic acid methyl ester (0.76 g) in 20% yield: HPLC R_t 8.77 min; mp 140 °C; IR 1720 cm^{-1} (acid carbonyl) and 1680 cm^{-1} (aryl carbonyl). Mass spectrum gave the molecular ion peak at m/z 392.

8-(2′-Fluoren-7′-butyl)-7-oxooctanoic acid methyl ester (0.4 g, 1.0 mmol) was dissolved in toluene (13 mL) and added to a 250-mL round bottom flask containing freshly prepared zinc amalgam (2.0 g, 1:4 molar ratio; w/w) in concentrated hydrochloric acid (5 mL). The reaction mixture was refluxed for 8 h when another aliquot of concentrated hydrochloric acid (5 mL) was added. Both the layers were separated, and the aqueous layer was extracted with ether. Both the toluene and ether layers were mixed, washed with water and saturated solution of sodium chloride, and dried over anhydrous sodium sulfate. Excess ether was distilled off on a water bath, and toluene was removed by vacuum distillation. The residue so obtained was subjected to silica gel (10 g) column chromatography and eluted with 30% chloroform in petroleum ether to get 8-(2′-fluoren-7′-butyl)octanoic acid methyl ester (0.22 g, 0.6 mmol) in 56% yield: HPLC R_t 21.05 min; IR 1740 cm^{-1} (ester carbonyl). Mass spectrum gave the molecular ion peak at m/z 378 and base peak at m/z 179 corresponding to fluorenyl $CH_2^{\bullet+}$ ion.

8-(2′-Fluoren-7′-butyl)octanoic acid methyl ester (0.19 g, 0.50 mmol) was dissolved in 10% methanolic potassium hydroxide (15 mL), and the reaction mixture was refluxed for 6 h. The reaction mixture was then concentrated to 5 mL and poured into water, followed by the neutralization with hydrochloric acid. The precipitated acid was filtered and dried under vacuum. The residue was crystallized from benzene–petroleum ether mixture to give pure 8-(2′-fluoren-7′-butyl)-octanoic acid (C8A-FL-C4; 0.18 g) in 98% yield: mp 120 °C; IR 1710 cm^{-1} (acid carbonyl); NMR ($CDCl_3$) δ 0.94 [t, 3 H, J = 7.3 Hz, CH_3–$(CH_2)_3$–], 1.36 [m, 8 H, CH_3–CH_2–$(CH_2)_2$– and HOOC–CH_2–CH_2–$(CH_2)_3$–CH_2–], 1.64 [m, 6 H, CH_3–CH_2–CH_2–CH_2– and HOOC–CH_2–CH_2–$(CH_2)_3$–CH_2–], 2.3 [t, 2 H, J = 7.6 Hz, HOOC–CH_2–$(CH_2)_2$–], 2.64 [m, 4 H, CH_3–$(CH_2)_2$–CH_2– and HOOC–$(CH_2)_6$–CH_2–], 3.82 (s, 2 H, C_9-H of fluorene), 7.15 (d, 2 H, J = 7.3 Hz, C_4 and C_5 of fluorene), 7.32 (s, 2 H, C_1 and C_8 of fluorene), 7.63 (d, 2 H, J = 7.78 Hz, C_3 and C_6 of fluorene). Mass spectrum gave the molecular ion peak at m/z 364, which was also the base peak.

6-(2′-Fluoren-7′-hexyl)hexanoic Acid (VIII, C6A-FL-C6). Fluorene (3.54 g, 21.2 mmol) was dissolved in dry carbon

[1] Abbreviations: C4A-FL, 4-(2′-fluorenyl)butyric acid; C6A-FL, 6-(2′-fluorenyl)hexanoic acid; C8A-FL, 8-(2′-fluorenyl)octanoic acid; C4A-FL-C4, 4-(2′-fluoren-7′-butyl)butyric acid; C6A-FL-C2, 6-(2′-fluoren-7′-ethyl)hexanoic acid; C6A-FL-C4, 6-(2′-fluoren-7′-butyl)hexanoic acid; C6A-FL-C6, 6-(2′-fluoren-7′-hexyl)hexanoic acid; C8A-FL-C4, 8-(2′-fluoren-7′-butyl)octanoic acid; 9,10-DBSA, 9,10-dibromostearic acid; DML, dimyristoyl phosphatidylcholine; NATA, *N*-acetyltryptophanamide; PC, phosphatidylcholine; TLC, thin layer chromatography.

disulfide (18 mL) and stirred. Anhydrous aluminum chloride (5.7 g, 42.4 mmol) was then added in portions. Freshly prepared caproic anhydride (5 g, 23.3 mmol) in dry carbon disulfide (10 mL) was added dropwise over a period of 1 h and then refluxed for the next 6 h. The excess of carbon disulfide was distilled, and the complex was washed with dry petroleum ether. The aluminum chloride complex was then hydrolyzed by addition into ice-cold dilute hydrochloric acid, stirred at room temperature for 4 h to ensure complete hydrolysis, and then extracted with chloroform. The chloroform layer was washed with 10% sodium bicarbonate solution, water, and saturated solution sodium chloride. Excess chloroform was distilled off on a water bath, and crude material so obtained was subjected to column chromatography over silica gel (450 g) and eluted out in 50% benzene in petroleum ether to give a crude material, which was crystallized from methanol to obtain pure 2-*n*-hexanoyl fluorene (14 g) in 65% yield: mp 117–118 °C; IR 1680 cm^{-1} (aryl carbonyl).

2-*n*-Hexanoyl fluorene (13.5 g, 51.1 mmol) was dissolved in toluene (200 mL) and added to a 1-L round bottom flask containing freshly prepared zinc amalgam (30 g, 1:6 molar ratio, w/w) in concentrated hydrochloric acid (150 mL). The reaction mixture was then refluxed for 8 h, when another lot of concentrated hydrochloric acid (100 mL) was added. Both the layers were separated, and the aqueous layer was extracted with ether. Both the toluene and the ether layers were mixed, washed with water and saturated solution of sodium chloride, and dried over anhydrous sodium sulfate. Excess ether was distilled on a water bath, and the toluene was removed by vacuum distillation. The residue so obtained was subjected to column chromatography over silica gel (150 g) and eluted in 25% chloroform in petroleum ether to give a crude material, which was crystallized from petroleum ether–methanol to obtain pure 2-*n*-hexylfluorene (8.07 g) in 61% yield: HPLC R_t 16.68 min; mp 59–60 °C; NMR ($CDCl_3$) δ 0.93 ppm [t, 3 H, $-(CH_2)_5-CH_3$], 1.38 [m, 8 H, $-CH_2-(CH_2)_4-CH_3$], 2.7 [t, 2 H, $-CH_2-(CH_2)_4-CH_3$], 3.88 (s, 1 H, C-9 of fluorene), 7.25–7.78 (m, 7 H, aromatic protons). Mass spectrum gave the molecular ion peak at m/z 250.

2-*n*-Hexylfluorene (4 g, 16.0 mmol) was acylated with methyl adipoyl chloride using anhydrous aluminum chloride, essentially by the procedure used for acylating 2-*n*-butylfluorene described in the previous section. The crude material was subjected to silica gel (105 g) column chromatography, and the desired product was eluted with 5% ethyl acetate in chloroform. Crystallization from benzene in petroleum ether gave pure 6-(2′-fluoren-7′-hexyl)-5-oxohexanoic acid methyl ester (2.2 g) in 35% yield: HPLC R_t 12.3 min; mp 100 °C; IR 1720 cm^{-1} (ester carbonyl) and 1680 cm^{-1} (aryl carbonyl); NMR ($CDCl_3$) δ 0.99 ppm [t, 3 H, $-(CH_2)_5-CH_3$], 1.2–3.2 [m, 18 H, $-(CH_2)_5-CH_3$ and $-CO-(CH_2)_4-COOCH_3$], 3.7 [s, 3 H, $-CO-(CH_2)_4-COOCH_3$], 3.95 (s, 2 H, C_9-H of fluorene), 7.2–8.2 (m, 6 H, aryl protons). Mass spectrum gave the molecular ion peak at m/z 392 and base peak at m/z 277 corresponding to the acylium ion.

6-(2′-Fluoren-7′-hexyl)-5-oxohexanoic acid methyl ester (1.6 g, 4.1 mmol) was subjected to Clemensen reduction with freshly prepared zinc amalgam as described in the previous section. The crude material so obtained was subjected to silica gel column chromatography and eluted with 25% chloroform in petroleum ether to get 6-(2′-fluoren-7′-hexyl)hexanoic acid methyl ester in 65% yield: HPLC R_t 24.33 min; mp 60 °C; IR 1730 cm^{-1} (ester carbonyl). Mass spectrum gave the molecular ion peak at m/z 378 which was also the base peak. Hydrolysis of the ester gave a solid which was crystallized from a benzene–hexane mixture to get pure 6-(2′-fluoren-7′-hexyl)hexanoic acid (C6A-FL-C6) in 94% yield: mp 122 °C; IR 1700 cm^{-1} (acid carbonyl); NMR ($CDCl_3$) δ 0.9 [t, 3 H, J = 7 Hz, $CH_3-(CH_2)_3-$], 1.3–1.5 [m, 8 H, $CH_3-(CH_2)_2-(CH_2)_3-$ and $HOOC-CH_2-(CH_2-)_2-$], 1.58–1.75 (m, 6 H, $CH_3-CH_2-CH_2-CH_2-CH_2-$ and $HOOC-CH_2-CH_2-CH_2-CH_2-CH_2-$), 2.35 [t, 2 H, J = 7.5 Hz, $HOOC-CH_2-(CH_2)_2-$], 2.6–2.7 [m, 4 H, $HOOC-(CH_2)_4-CH_2-$ and $CH_3-(CH_2)_4-CH_2-$], 3.82 (s, 2 H, C_9-H of fluorene), 7.16 (d, 2 H, J = 7.76 Hz, C_4 and C_5 of fluorene), 7.3 (s, 2 H, C_1 and C_8 of fluorene), 7.63 (d, 2 H, J = 7.78 Hz, C_3 and C_6 of fluorene). Mass spectrum gave the molecular ion peak at m/z 364, which was also the base peak.

HPLC and GC analysis was carried out for all acids including the normal fatty acids. It was observed that under similar conditions of elution the retention time for the fluorenyl fatty acids increases with increase in chain length of the fatty acid chain. It was seen that C4A-FL-C4 (II) has a retention time similar to that of C8A-FL (III), possibly as a result of the fact that both acids have a similar carbon atom chain length. C6A-FL-C6 (VIII) and C8A-FL-C4 (IV) elute at the longest retention times because of the greater hydrophobic interaction with the C18 chain of the ODS column.

Fluorescence Studies. All solvents used were of spectroscopy grade from Merck, Bombay (India). Fluorescence spectra were recorded on a Shimadzu RF 540 fluorescence spectrometer. All fluorescence intensity measurements were corrected for dilution and light scattering. Fluorescence excitation and emission spectra were recorded by setting emission and excitation wavelengths at 272 and 315 nm, respectively. The excitation and emission slits were 5 and 5 nm, respectively. Fluorescence quantum yield measurements were carried out in methanol using *N*-acetyltryptophanamide (NATA) as the standard (ϕ = 0.15 in double-distilled water) (Kirby & Steiner, 1970). Care was taken to maintain the OD of all samples at the excitation wavelength to a value of less than 0.25, thus avoiding any inner filter effects while recording the fluorescence emission spectra. Quantum yields were calculated using (Schulman, 1977)

$$F_2/F_1 = \text{area}_2/\text{area}_1 = (\phi_2/\phi_1)(OD_2/OD_1)$$

where F is the fluorescence intensity, area refers to the area under the fluorescence curve, ϕ is the quantum yield, and OD is optical density. 1 and 2 in the subscripts indicate sample and standard, respectively.

Phosphatidylcholine (PC) vesicle samples were prepared by sonication as described earlier (Lala et al., 1988), the PC concentration in these vesicle preparations being 0.5 mM. An aliquot of 2 mM solution of the fluorenyl fatty acids in methanol was added to the vesicles so that the final PC to fluorenyl fatty acid molar ratio was 250:1 and the methanol concentration 0.12% (v/v). The vesicle preparation was then incubated at 25 °C for 45 min.

Whole blood was obtained from IIT Hospital. The buffers used were PBS (5 mM phosphate buffer, 150 mM NaCl, pH 7.4) and phosphate–EDTA buffer (5 mM phosphate buffer containing 1 mM EDTA, pH 8).

Isolation of Erythrocyte Ghost Membranes. Human erythrocyte ghosts were isolated from freshly or recently outdated blood by the method of Steck and Kant (1974). Briefly, blood was centrifuged at 5000*g* and a buffy coat of leucocytes was separated from the red blood cells. A pellet of red blood cells obtained was repeatedly washed with phosphate-buffered saline (5 mM phosphate, 150 mM NaCl, pH 7.4). The cells were then subjected to hypotonic lysis using phosphate–EDTA buffer. After repeated washing with this

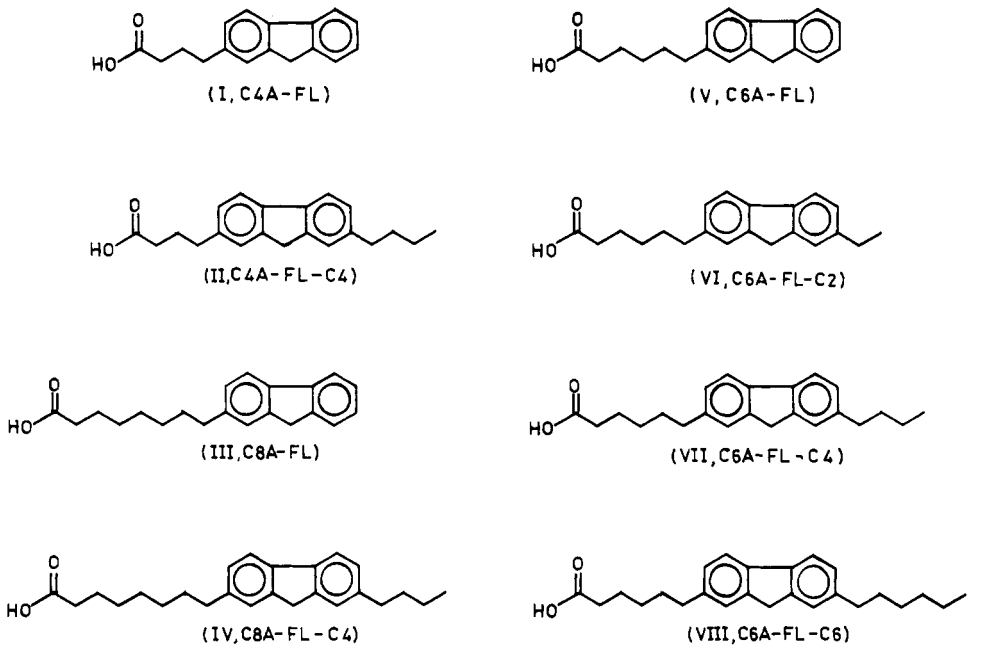

FIGURE 1: Structure of fluorenyl fatty acids.

buffer at 12000g, the ghosts were obtained as a soft pellet. The protein concentration was then estimated by the method of Markwell et al. (1981). Ghosts were stored at −20 °C and used within a maximum of 3 days. However, most experiments were conducted immediately after isolation of the ghosts to avoid intrinsic proteolysis in ghosts.

Preparation of Resealed Vesicles from Erythrocyte Ghosts. Resealed right-side-out vesicles were prepared by taking the ghost membrane pellet obtained earlier in phosphate-buffered saline (PBS) pH 8 and incubating at a temperature of 37 °C for a minimum of 1 h (Luxnat & Joachim, 1986).

Fluorescence Studies of Fluorenyl Fatty Acids in Erythrocyte Ghost Membranes. Washed ghosts (4 mg of protein/mL) were taken in aliquots and diluted to 1 mL with phosphate buffer (final protein concentration was 150 μg). 4.5 μL of 2 mM fluorenyl fatty acid probe solutions in methanol was then added to the ghost samples and incubated for 1 h for the probes to partition into the membrane. The samples were then spun on a microfuge for 1 min, and the pellet obtained was again washed with 1 mL of buffer. The pellet was then diluted to 6 mL, and emission spectra of these samples were recorded. Measurements were also done on a membrane sample not containing any probe to get the membrane intrinsic fluorescence. The supernatant and washings were collected and pooled for each of the samples, and the emission intensity was recorded for these samples along with the actual membrane samples for evaluating the efficiency of partitioning of each probe molecule into the membrane after making suitable corrections.

Quenching of Fluorenyl Fatty Acid Probes in Egg PC Vesicles and Erythrocyte Ghosts. A 4 M solution of KI containing a small amount of 10 mM $Na_2S_2O_3$ solution added to reduce the formation of I_2 and I_3^- was used for iodide quenching studies. Small aliquots (8 μL) of a 4 M solution of KI were added successively to the vesicle preparation, and emission spectra were recorded. Similarly, in the case of 9,10-dibromostearic acid, a 5.4 mM solution in methanol was used for the quenching studies. Small aliquots (4 μL) were added successively to the PC vesicle preparation. After each addition of the 9,10-dibromostearic acid, the sample was incubated for 45 min at 25 °C to ensure uptake of the quencher before recording the emission spectrum. Resealed erythrocyte ghosts, right-side-out vesicles, were used for fluorescence quenching studies. Samples containing the fluorenyl fatty acid probes were partitioned into resealed erythrocyte ghost vesicles (protein concentration, 25 μg/mL) as mentioned above in the case of erythrocyte ghost membrane. Small aliquots (4 μL) of a 5.4 mM solution of 9,10-dibromostearic acid in methanol were added successively to the samples, which were then incubated for 45 min before taking the reading. Fluorescence spectra were recorded with an excitation wavelength of 272 nm. The excitation and emission slits were 5 and 10 nm, respectively.

Fluorescence Polarization Studies. PC vesicles were prepared and incubated with fluorenyl fatty acids as described earlier. Fluorescence polarization data at 20 °C were obtained by setting the excitation and emission wavelengths at 272 and 315 nm, respectively. The excitation and emission slits were 5 and 10 nm, respectively. Polarization studies of these fatty acid probes were also carried out in dimyrisitoyllecithin (DML) vesicles below (20 °C) and above (35 °C) the transition temperature of DML. DML vesicles were prepared in a similar fashion as egg PC vesicles. The final phospholipid concentration (DML) was 0.5 mM, and the phospholipid to probe molar ratio was 250:1. Resealed right-side-out erythrocyte ghosts samples were prepared in a similar fashion as described in the quenching studies. Measurements were also done for ghost membranes without any probe. All measurements with ghost membranes were carried out at 25 °C. Corrections for scatter were also done by measuring the polarization values for blank samples. The polarization measurements and calculations were carried out as described earlier (Lala et al., 1988).

RESULTS

Fluorenyl fatty acids reported here, 6-(2′-fluoren-7′-ethyl)hexanoic acid (C6A-FL-C2), 6-(2′-fluoren-7′-butyl)-hexanoic acid (C6A-FL-C4), 6-(2′-fluoren-7′-hexyl)hexanoic acid (C6A-FL-C6), and 8-(2′-fluoren-7′-butyl)octanoic acid (C8A-FL-C4) (Figure 1) were prepared essentially according to the procedure reported earlier (Lala et al., 1988), i.e., Friedel–Crafts acylation of acetylfluorene, *n*-butylfluorene, and *n*-hexylfluorene with the respective fatty acid chlorides, followed by Clemensen reduction of the intermediate keto-

Table I: Absorption and Emission Characteristics of the Fluorenyl Fatty Acid Probes

probe	absorbance (ϵ)[a]			emission maxima (nm)[b]	ϕ[c]
C4A-FL-C4	272 (2700)	297 (8250)	308 (10450)	320	0.56
C6A-FL-C4	271 (37500)	296 (12500)	308 (15000)	316	0.62
C6A-FL-C6	270 (22450)	297 (11260)	309 (13134)	319	0.68
C8A-FL-C4	270 (37996)	297 (10976)	309 (15038)	319	0.65

[a] Absorption values in nanometers recorded in methanol. The molar extinction coefficient (M^{-1} cm^{-1}) are given in parentheses below the individual wavelengths. [b] Fluorescence emission was recorded in methanol, and the wavelength of excitation was 272 nm. [c] Fluorescence quantum yield was measured in methanol, and NATA (ϕ = 0.15 in double-distilled water) was used as a standard.

esters. All the fluorenyl fatty acids obtained were purified to homogeneity as indicated by TLC and HPLC analysis. Further, the spectral characteristics fully corroborated the structure of the fluorenyl fatty acids reported here. The absorption spectra of these fatty acids gave prominent bands around 270, 300, and 310 nm (Table I). As reported earlier (Lala et al., 1988), the excitation spectrum of these fatty acids in methanol gives a maxima around 272 nm, whereas the emission maxima appears around 320 nm. These probes do not show any variation in the emission maxima in different solvents like hexane, chloroform, and methanol. It is observed that these fluorenyl fatty acid probes have a high fluorescence quantum yield (Table I) and can thus be used at low concentrations to study membranes. The fluorenyl fatty acids could be conveniently partitioned into egg phosphatidylcholine (PC) vesicles by incubation at 25 °C for 45 min, wherein excitation and emission spectra similar to that in methanol were observed. The high quantum yield permitted working at PC to probe molar ratio of 250:1. In order to study the partitioning of these probes in PC vesicles containing any fluorenyl fatty acid at 250:1 molar ratio, the vesicle preparation was passed over a Sephadex G-25 column. Fluorescent analysis of the eluant indicated that all fluorenyl fatty acid was associated with the PC vesicles which appear in the void volume. A control experiment without the PC vesicles indicated that free fluorenyl fatty acids elute much after the void volume. Thus at the concentration of PC (0.5 mM) and fluorenyl fatty acids (2 μM) used in all studies reported here, these probes completely partition into the vesicles.

Fluorescence Quenching Studies in Artificial Membranes. The orientation of fluorescent probes in membranes can be best studied by following the depth-dependent quenching of their fluorescence in membranes (Blatt & Sawyer, 1985). Both water-soluble quenchers like iodide and Cu (II) (Thulborn & Sawyer, 1978; Lala, et al., 1988; De Kroon et al., 1990) and lipid-soluble quenchers like brominated fatty acids and phospholipids (East & Lee, 1982; Lala & Koppaka, 1989; Bolen & Holloway, 1990; De Kroon et al., 1990) have been used toward this end. The fluorescence quenching process can be described by the Stern–Volmer equation:

$$(I_o/I) - 1 = K_{sv}[Q]_T = k_q\tau[Q]_T \quad (1)$$

where I_o and I are fluorescence intensities before and after addition of the quencher, K_{sv} is the Stern–Volmer constant (Stern & Volmer, 1919), k_q is the bimolecular quenching constant, τ the fluorescence lifetime of the fluorophore in

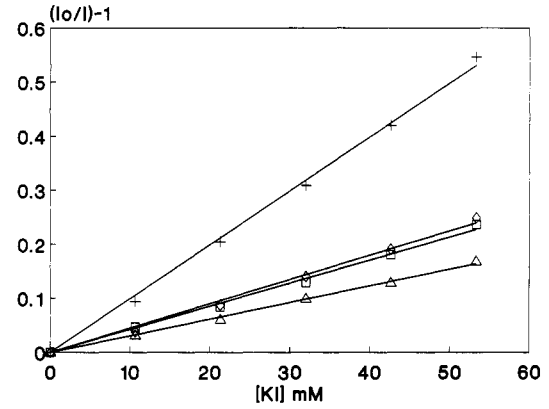

FIGURE 2: Stern–Volmer plots for the quenching of fluorenyl fatty acids C6A-FL (+), C6A-FL-C4 (□), C8A-FL (◇), and C8A-FL-C4 (△) bound to PC vesicles, by KI. The PC concentration in the vesicle preparation was 0.5 mM. The PC to probe molar ratio was 250:1. The excitation wavelength was 272 nm, and emission was monitored at 315 nm. I_o is the fluorescence intensity in the absence of quencher, and I is the intensity in the presence of quencher.

absence of the quencher, and $[Q]_T$ is the total concentration of the quencher added. A plot of $(I_o/I) - 1$ versus $[Q]_T$ gives a linear plot passing through the origin. A higher slope (K_{sv}) indicates proximity of the quencher to the fluorescent chromophore. Thus, if the position of a quencher can be determined, e.g., as has been done in the case of phospholipids prepared from brominated fatty acids by X-ray diffraction (McIntosh & Holloway, 1987), the position of the fluorophore can be estimated. Attempts have also been made to get distance information using this approach (Chattopadhyay & London 1987; Bolen & Holloway, 1990). In brief, a higher slope (K_{sv}) in the Stern–Volmer plot indicates a greater proximity of the fluorophore to the quencher.

Iodide has been successfully used for quenching studies in membranes. Iodide being highly water soluble, it very poorly partitions into the apolar environment of the membrane bilayer. However, at higher concentrations a few ions penetrate the bilayer leading to higher quenching of the shallow fluorescent probes compared to the deeper probes (Chalpin & Kleinfeld, 1983). Figure 2 gives the Stern–Volmer quenching plots for iodide quenching of ordinary (C6A-FL, C8A-FL) and tailed fluorenyl fatty acids (C6A-FL-C4 and C8A-FL-C4) incorporated in PC vesicles. In both cases the tailed fatty acids were quenched much less than the ordinary fluorenyl fatty acids. However, the decrease in quenching becomes less pronounced with increase in length of fluorenyl fatty acid (Table II). This is not surprising in view of the fact that very few ions would penetrate 8–10 carbon atoms from the membrane–water interface.

9,10-Dibromostearic acid has been effectively used as a quencher for studies in membrane (Jain & Maliwal, 1985; Lala & Koppaka, 1989). Figure 3 gives the Stern–Volmer plots for the quenching of the fluorenyl fatty acids in PC vesicles by 9,10-dibromostearic acid. The values obtained for the quenching constants are given in Table II. It is once again observed that the tailed compounds are quenched much more relative to the ordinary fluorenyl fatty acids. The quencher being intrinsic and located deep in the membrane, the difference in K_{sv}'s seems much more pronounced with fluorenyl fatty acids like C8A-FL/C8A-FL-C4 relative to C4A-FL/C4A-FL-C4. These data clearly indicate that attachment of the hydrophobic tail certainly assists in better alignment of the fluorenyl fatty acids. In a fully extended conformation, the tailed and the untailed ordinary fluorenyl fatty acids should probe the membrane at similar depths. However, the deeper

Table II: Stern–Volmer (K_{SV}) Quenching Constants Determined for the Quenching of Fluorenyl Fatty Acids by KI and 9,10-Dibromostearic Acid (9,10-DBSA) and Fluorescence Polarization (P) Data in PC Vesicles and Erythrocyte Ghosts (Right-Side-Out Vesicles)

	PC vesicles			erythrocytes (ROV)	
probe	K_{SV} (M^{-1}) KI	K_{SV} (M^{-1}) 9,10-DBSA	polarization (P)	K_{SV} (M^{-1}) 9,10-DBSA	polarization (P)
C4A-FL	12.45	3562	0.028	6119	0.01
C4A-FL-C4	4.31	26015	0.154	21628	0.146
C6A-FL	9.48	12482	0.072	13064	0.03
C6A-FL-C4	4.06	32139	0.154	74120	0.202
C6A-FL-C6	3.79	34233	0.168	98725	0.233
C8A-FL	4.30	26719	0.09	26030	0.093
C8A-FL-C4	2.93	37123	0.15	135137	0.209

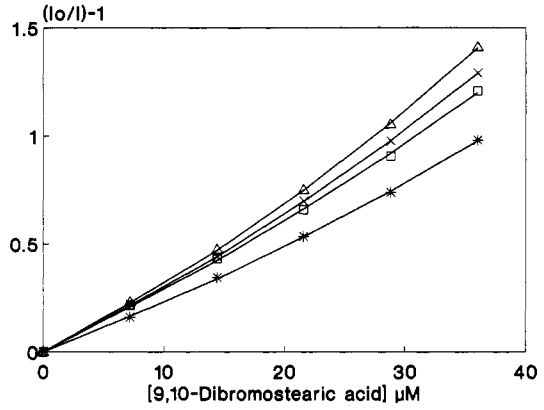

FIGURE 3: Stern–Volmer plots for the quenching of fluorenyl fatty acids C4A-FL-C4 (*), C6A-FL-C4 (□), C6A-FL-C6 (×), and C8A-FL-C4 (△) bound to PC vesicles, by 9,10-dibromostearic acid. All other conditions are as described in the legend to Figure 2.

location of the tailed fluorenyl fatty acids (C4A-FL-C4, C6A-FL-C4, C8A-FL-C4) indicated by two independent quenchers shows that these compounds provide a more appropriate depth-dependent analysis whereas the untailed ordinary fluorenyl fatty acids (C4A-FL, C6A-FL, C8A-FL) undergo rather large wobbling motion, leading to an inappropriate depth-dependent analysis of the membrane.

In order to see the effect of length of the hydrophobic tail on the orientation of fluorenyl fatty acid probes in membranes, four compounds were tested wherein the C6A-FL has a two-, four-, or six-carbon-atom tail, i.e., C6A-FL-C2, C6A-FL-C4, and C6A-FL-C6. Incorporation of these compounds in membranes followed by quenching studies with 9,10-dibromostearic acid indicated that the C4 tail is sufficient for effective alignment of fluorenyl fatty acids in membranes.

Fluorescence Studies of Fluorenyl Fatty Acids in Erythrocyte Ghosts. All the fluorenyl fatty acids could be easily incorporated into erythrocyte ghost membranes by incubation for 1 h. In order to see if these probes are fully incorporated in the erythrocyte as observed with PC vesicles, the incubated preparation was centrifuged. Analysis of the pellet and the supernatant by measuring the fluorescence intensity at 315 nm indicated that, with the exception of short-chain fluorenyl fatty acids like C4A-FL, all other fatty acids were incorporated to around 80%. In order to minimize the possibility of any free probe, all studies were conducted after resuspending the centrifuged ghost pellet in buffer. During the course of the experiment no substantial leakage of the probes from the ghost could be detected. Figure 4 gives the emission spectra of the fluorenyl fatty acids C8A-FL and C4A-FL-C4 in erythrocyte ghost membranes. As can be clearly seen, the tryptophans from the erythrocyte ghost protein do not make any major contribution to the overall fluorescence of fluorenyl fatty acids. This is not surprising because the quantum yield of the fluorenyl fatty acids (≈0.7) is much higher compared to that of tryptophan (≈0.15) (Table I).

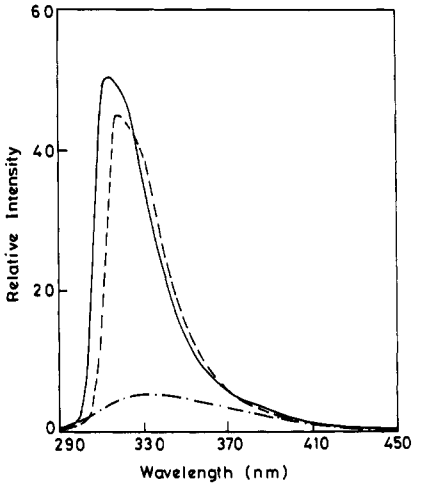

FIGURE 4: Fluorescence emission spectra of C8A-FL (—) and C4A-FL-C4 (---) in human erythrocyte ghost membranes. The concentration of the erythrocyte membrane protein was 25 μg/mL in PBS, pH 7.4. The excitation wavelength used was 272 nm. The fluorescence emission spectra of the ghost membranes (-·-) is also shown for comparison.

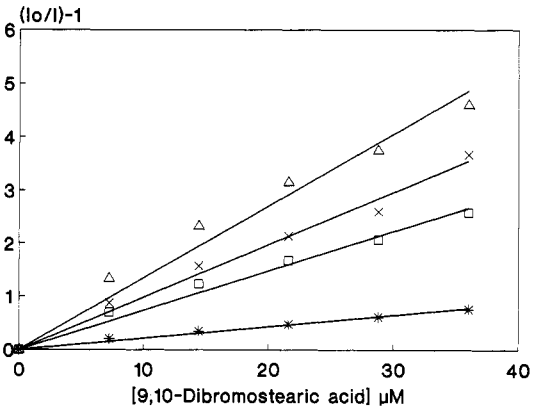

FIGURE 5: Stern–Volmer plots for the quenching of fluorenyl fatty acids C4A-FL-C4 (*), C6A-FL-C4 (□), C6A-FL-C6 (×), and C8A-FL-C4 (△) bound to human erythrocyte ghost membranes (right-side-out vesicles), by 9,10-dibromostearic acid. I_0 is the fluorescence intensity in the absence of the quencher, and I is the intensity in the presence of the quencher.

Fluorescence Quenching Studies in Erythrocyte Ghost Membranes. The fluorenyl fatty acids incorporated in the erythrocyte ghosts were subjected to fluorescence quenching studies using 9,10-dibromostearic acid as described earlier in the case of artificial membranes. The ordinary fluorenyl fatty acids (C4A-FL, C6A-FL, C8A-FL) without hydrophobic tails are quenched to a much lower degree compared to the corresponding fluorenyl fatty acids with tails (C4A-FL-C4, C6A-FL-C4, C6A-FL-C6, C8A-FL-C4) (Figure 5). It is interesting to note here that the change in K_{sv} on going from ordinary untailed fluorenyl fatty acids to tailed fatty acids shows the opposite trend to that observed in artificial mem-

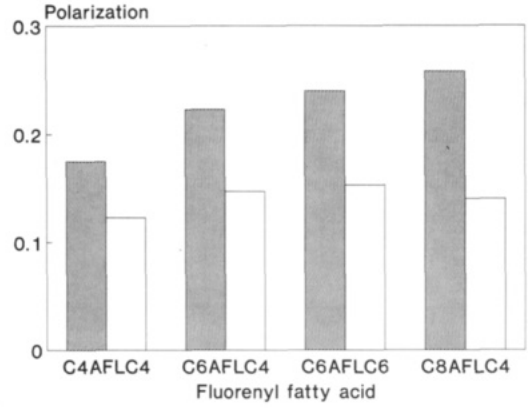

FIGURE 6: Fluorescence polarization data for tailed fluorenyl fatty acids in DML vesicles below (20 °C, shaded bar) and above (35 °C, unshaded bar) the phase transition.

branes (Table II). While the C4A-FL-C4 was much more strongly quenched relative to C4A-FL in PC vesicles, it is the C6A-FL-C4 and C8A-FL-C4 which are quenched much more compared to their untailed analogues. The increase in change in K_{sv} for C4A-FL compared to C6 and C8 can be attributed to the sharp curvature in PC vesicle relative to ghost membrane preparation.

Fluorescence Polarization Studies. Fluorescence polarization of these probes was determined in egg PC vesicles. The polarization data (Table II) clearly indicate that the tailed compounds (C4A-FL-C4, C6A-FL-C2, C6A-FL-C4, C6A-FL-C6, C8A-FL-C4) are more strongly immobilized than the untailed ones. Fluorescence polarization of these fluorenyl fatty acids in human erythrocyte ghosts was also determined. These data (Table II) also indicate that the tailed fatty acids indeed have a much higher polarization value, and the trend is very similar to the one observed in the case of egg PC vesicles. The increase in polarization seems to be more pronounced in the case of C4 than in the case of longer chain fatty acids, C6 and C8, suggesting that it is more important to have a hydrophobic tail attached to shorter chain fatty acids.

In order to see if these fatty acids can interdigitize with the opposite monolayer of the membrane, fluorescence polarization studies were conducted both in the gel (20 °C) and liquid-crystalline (35 °C) state of DML vesicles. At 35 °C the trend in the polarization (Figure 6) is found to be very similar to the one seen in egg PC (Table II). However, in the gel state, where the interdigitation with the opposite leaflet of the bilayer is more predominant (Nambi et al., 1988), significantly different values for polarization were obtained. The values for polarization seem to be larger in the case of longer chain fatty acids, i.e., C8A-FL-C4.

These compounds can also be effectively used to study phase transitions in membranes. Figure 7 shows the effect of temperature on the fluorescence polarization values of both C6A-FL-C6 and C8A-FL-C4 in DML vesicles. It is observed that the polarization value decreases with increase in temperature. The plots show the transition temperature of DML vesicles to be around 25 °C using both the fluorenyl fatty acids.

Discussion

The main objective of depth-dependent analysis of membranes is to provide structural information at different positions in the hydrophobic core. A variety of fluorescent probes, e.g., *n*-anthroyloxy fatty acids (Thulborn & Sawyer, 1978), have been used in this context. In order to be effective, it is essential to ensure that these probes are aligned properly so as to cause minimal perturbation to membranes. However, any probe by

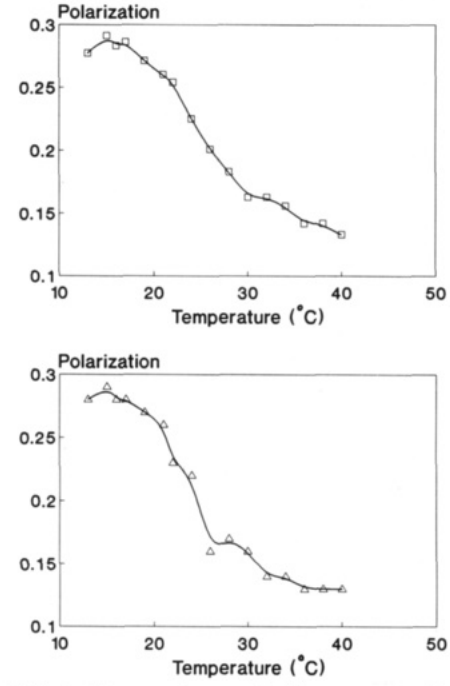

FIGURE 7: Effect of temperature on the fluorescence polarization of C6A-FL-C6 (top, □) and C8A-FL-C4 (bottom, △) when bound to DML vesicles.

definition will cause some perturbation, and one can only attempt to minimize these perturbations. Thus attachment of a fluorescent chromophore to fatty acids has been done recently via methylene linkages, e.g., pyrene (Waka et al., 1980; Jones & Lentz, 1986), anthracene (de Bony & Tocanne, 1983; Vincent et al., 1985; Molotkovsky, 1984), and fluorene (Lala et al., 1988), instead of ester linkages used in early studies (Thulborn & Sawyer, 1978). The wealth of information made available by use of fluorescent probes often leads to less emphasis being paid to molecular design of these probes. Thus the number of papers on use of fluorescent probes in membranes far outnumber the reports dealing with design of these probes, and it is only recently that attention has been drawn to effective molecular design of these probes (Silvius, 1990). The present work indicates that, with appropriate molecular design (Lala et al., 1988), better probes can be prepared. Thus attachment of a hydrophobic tail to different fluorenyl fatty acids leads to a much better alignment of the fluorescent probes in a membrane as indicated by fluorescence quenching and fluorescence polarization studies. Despite our initial apprehensions regarding use of fluorenyl fatty acids as fluorescent probes in natural membranes in view of excitation wavelength being 272 nm (Lala et al., 1988), the high quantum yield of fluorene ensured that these probes can also be successfully used for studying natural membranes like human erythrocytes.

Table II indicates that attachment of a *n*-butyl chain as a hydrophobic tail to the three fluorenyl fatty acids (C4A-FL, C6A-FL, C8A-FL) leads to a higher degree of quenching by 9,10-dibromostearic acid in both artificial and natural membranes. However, the increase in quenching on attachment of a hydrophobic tail is more pronounced in the case of shallow probe, C4A-FL, in artificial membranes, indicating that in small unilamellar vesicles the shorter chain fluorescent probes can undergo a large degree of wobbling motion. This wobbling motion can be stabilized by attachment of a hydrophobic tail. The effect is reversed in natural membranes like erythrocyte membrane. The large size of ghost membranes with practically no curvature constraint, as in the case of single unilamellar

vesicles, provides a more fluid environment deeper in the hydrophobic core. This leads to a better packing of shallower probes (C4A-FL) relative to deeper probes (C8A-FL), making it essential to attach a hydrophobic tail to deeper probes in natural membranes relative to shallower probes. It is, however, important to ensure that attachment of hydrophobic tail to deeper probes does not lead to such an increase in the overall length of the fatty acid probe that it starts penetrating into the other bilayer. This phenomena, referred to as interdigitation in the membrane bilayers, has been often observed (Harwood, 1989). It is unlikely that the fluorenyl fatty acids used here would be involved in interdigitation in PC vesicles or erythrocyte membranes. However, using single bilayer vesicles prepared from DML, significantly higher values of fluorescence polarization observed with C6A-FL-C6 and C8A-FL-C4 relative to other fluorenyl fatty acids (Figure 6) in the gel state indicates that these fatty acids interdigitize to some extent with the opposite bilayer in the gel state.

In conclusion, we feel that use of fluorescent fatty acids for depth-dependent analysis of membranes will benefit by use of hydrophobic tail based probes. These hydrophobic tails tend to stabilize the orientation of such probes in a membrane and thus provide information at a typical depth as predicted from their transverse location in a membrane. Finally, the results described with fluorenyl fatty acids as fluorescent probes also become significant in view of the fact that they can be converted to their diazofluorene analogues (Lala et al., 1989), a reagent which has been effectively used for membrane hydrophobic core labeling (Pradhan & Lala, 1987).

Registry No. I, 7250-03-5; II, 116996-80-6; III, 116971-37-0; IV, 141046-20-0; V, 116971-36-9; VI, 122911-54-0; VII, 141046-21-1; VIII, 141046-22-2; 2-*n*-butylfluorene, 42946-58-7; methyl suberoyl chloride, 41624-92-4; 8-(2′-fluoren-7′-butyl)-7-oxooctanoic acid methyl ester, 141046-23-3; fluorene, 86-73-7; caproic anhydride, 2051-49-2; 2-*n*-hexanoylfluorene, 29021-11-2; 2-*n*-hexylfluorene, 99012-32-5; methyl adipoyl chloride, 35444-44-1; 6-(2′-fluoren-7′-hexyl)-5-oxohexanoic acid methyl ester, 141046-25-5.

References

Anjaneyulu, P. S. R., & Lala, A. K. (1988) *Indian J. Chem. 27B*, 1067–1068.

Blatt, E., & Sawyer, W. H. (1985) *Biochim. Biophys. Acta 822*, 43–62.

Bolen, E. J., & Holloway, P. W. (1990) *Biochemistry 29*, 9638–9643.

Buu-Hoi., & Cangihant, P. (1946) *Bull. Soc. Chim. Fr.*, 123–134.

Chalpin, D. B., & Kleinfeld, A. M. (1983) *Biochim. Biophys. Acta 731*, 465–472.

Chattopadhyay, A., & London, E. (1987) *Biochemistry 26*, 39–45.

de Bony, J., & Tocanne, J. F. (1983) *Chem. Phys. Lipids 32*, 105–121.

De Kroon, A. I. P. M., Soekarjo, M. W., De Gier, J., & De Kruijff, B. (1990) *Biochemistry 29*, 8229–8240.

East, J. M., & Lee, A. G. (1982) *Biochemistry 21*, 4144–4151.

Harwood, J. L. (1989) *Trends Biochem. Sci. 14*, 2–4.

Huang, M. (1946) *J. Am. Chem. Soc. 68*, 2487–2488.

Jain, M. K., & Maliwal, B. P. (1985) *Biochim. Biophys. Acta 815*, 135–140.

Jones, M. E., & Lentz, B. R. (1986) *Biochemistry 25*, 567–574.

Kirby, E. P., & Steiner, R. F. (1970) *J. Phys. Chem. 74*, 4480–4486.

Lala, A. K., & Koppaka, V., (1989) *Photochem. Photobiol. 49*, 763–767.

Lala, A. K., Dixit, R. R., Koppaka, V., & Patel, S. (1988) *Biochemistry 27*, 8981–8989.

Lala, A. K., Dixit, R. R., & Koppaka, V. (1989) *Biochim. Biophys. Acta 978*, 333–336.

Luxnat, M., & Joachim, H. (1986) *Biochim. Biophys. Acta 856*, 274–282.

Markwell, M. A. C., Hass, S. M., Tolbert, N. E., & Bieber, L. L. C. (1981) *Methods Enzymol. 72*, 296–303.

McIntosh, T. J., & Holloway, P. W. (1987) *Biochemistry 26*, 1783–1788.

Molotkovsky, J. G., Manevich, Y. M., Babak, V. I., & Bergelson, L. D. (1984) *Biochim. Biophys. Acta 778*, 281–282.

Nambi, P., Rowe, E. S., & McIntosh, T. J. (1988) *Biochemistry 27*, 9175–9182.

Perrin, D. D., Armarego, W. L. F., & Perrin, D. R. (1980) *Purification of Laboratory Chemicals*, Pergamon Press, Oxford.

Pradhan, D., & Lala, A. K. (1987) *J. Biol. Chem. 262*, 8242–8251.

Schulman, S. G. (1977) *Fluorescence and Phosphorescence Spectroscopy: Physicochemical Principles and Practice*, Pergamon Press, Oxford.

Silvius, J. R. (1990) *Biochemistry 29*, 2930–2938.

Steck, T. L., & Kant, J. A. (1974) *Methods Enzymol. 31*, 172–180.

Stern, O., & Volmer, M. (1919) *Z. Phys. 20*, 183–188.

Thulborn, K. R., & Sawyer, W. H. (1978) *Biochim. Biophys. Acta 511*, 125–140.

Vincent, M., Gallay, J., de Bony, J., & Tocanne, J. F. (1985) *Eur. J. Biochem. 150*, 341–347.

Waka, Y., Mataga, N., & Tanaka, F. (1980) *Photochem. Photobiol. 32*, 335–340.